Design tradeoffs in a synthetic gene control circuit for metabolic networks

Diego A. Oyarzún[⋆†] and Guy-Bart Stan[†]

***Abstract*— The performance of genetic control circuits for metabolism is subject to a number of tradeoffs that must be addressed at the design stage. We explore how the metabolic steady state and transient response depend on the regulatory topology and design parameters such as promoter and ribosome binding site strengths. We consider a one-to-all transcriptional control circuit for an unbranched metabolic pathway with saturable enzyme kinetics. The analysis highlights a compromise between operon and non-operon topologies in terms of robustness and design flexibility. We show that enzyme half-lives are an upper bound on the speed at which the pathway can adapt to a changing metabolic demand. We also analyze the destabilizing effect of basal enzyme expression and high regulatory sensitivity, albeit the latter reduces the steady state product bias.**

I. Introduction

Synthetic Biology aims at engineering cellular systems to perform customized and programmable biological functions. Since the seminal works in [1], [2], the design of synthetic gene modules with prescribed functionalities has undergone great progress [3]. Synthetic control of metabolism, however, is still in its infancy [4], as it requires a complex integration between the genetic and metabolic domains. This is an important bottleneck in Synthetic Biology, as one of its most prominent applications is the manipulation of bacterial metabolism to produce chemicals for sectors such as energy, biomedicine and food technology [5]. There is a substantial need for genetic control circuits that ensure robust pathway operation under changing environmental conditions, cell-to-cell variability and biochemical noise.

Two landmark implementations of engineered genetic-metabolic circuits are the control of lycopene production [6] and the metabolic oscillator described in [7]. Although it is clear that feedback control is crucial to achieve robust metabolic regulation, only few works have tackled the general design problem from a control-theoretic perspective. Notably, the work in [8] demonstrated the use of a synthetic toggle switch [2] as an ON-OFF controller for metabolism, whereas in [9] the authors explored different genetic control architectures for biofuel production.

In this paper we study an unbranched metabolic network under one-to-all transcriptional repression from the product. In a one-to-all architecture, product-responsive transcription factors (TF) regulate the expression of all pathway enzymes [10]. This feedback structure mimics natural circuits enabling cellular adaptations to environmental perturbations, e.g. in amino acid metabolism [11], [12]. Our goal is to identify the design tradeoffs that must be addressed, and how the chosen feedback structure limits performance under changes in product demand.

We consider a nonlinear ODE model for the feedback system that comprises kinetic equations for the metabolic species and product-dependent enzyme expression (§II). We observe that operon control (i.e. with genes regulated by a single TF) tends to be more robust than multiple TF control, but it is less flexible in that it yields uniform enzyme expression levels (§III). Linear analysis reveals that one-to-all control has the enzyme half-lives as fixed modes. Because these are much longer than metabolic time scales [13], they correspond to an upper bound on the transient response speed. We also find that leaky enzyme expression has a destabilizing effect, thereby inducing a stable limit cycle under high-sensitivity enzyme repression (§IV). Upon changes in product demand, the circuit response is subject to a tradeoff between its adaptation speed and the steady state product bias, but the latter can be curbed with a more sensitive feedback (§V).

II. Model description

We consider networks as the ones shown in Fig. 1, where s_0 denotes the concentration of substrate, s_1 is an intermediate metabolite, and s_2 is the metabolic product. The metabolic reactions occur at a rate v_i (each one catalyzed by an enzyme with concentration e_i), and d denotes the cellular demand rate for product.

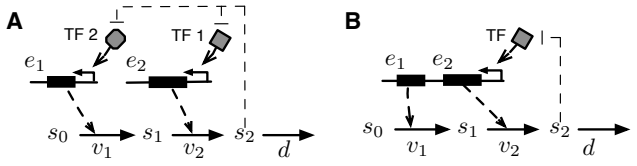

Fig. 1. One-to-all transcriptional repression of an unbranched metabolic pathway. Enzyme expression can be controlled by: (A) multiple TFs, or (B) a single TF controlling an operon.

A. Metabolic network

The network in Fig. 1 exchanges mass with the environment and/or other networks in the cell. The model accounts for this interaction via the input substrate s_0 and the output demand rate d. Because we are interested in biologically meaningful phenotypes, we assume that s_0 is constant to ensure that the network can reach a nonzero steady state [14]. The constant substrate assumption is also suitable for

⋆ Corresponding author, d.oyarzun@imperial.ac.uk.

† Centre for Synthetic Biology and Innovation, Department of Bioengineering, Imperial College London, SW7 2AZ United Kingdom.

scenarios where s_0 is an extracellular substrate pool shared by a low density cell population (so that the effects of cell-to-cell competition are negligible).

In a pathway with n reactions and n metabolites, the rate of change of metabolite concentrations can be described by

$$\dot{s}_i = v_i(s_{i-1}, e_i) - v_{i+1}(s_i, e_{i+1}), \tag{1}$$

for $i = 1, 2, \ldots, n$ and $v_{n+1} = d$. This model arises from the mass balance between the reactions that produce and consume s_i, and the enzyme kinetics are comprised in the reaction rates $v_i(s_{i-1}, e_i)$. To keep the analysis as general as possible, we will not presuppose a specific form for the enzyme kinetics. Instead we will generically assume that the metabolic reaction rates are linear in the enzyme concentrations [13]:

$$v_i(s_{i-1}, e_i) = g_i(s_{i-1})e_i, \tag{2}$$

where g_i is the enzyme turnover rate (i.e. the reaction rate per unit of enzyme concentration). We will also assume that the enzyme turnover rates are increasing and saturable functions of the metabolite concentrations, so that

$$g_i'(s_{i-1}) > 0, \tag{3}$$

and

$$\lim_{s_{i-1}\to\infty} g_i(s_{i-1}) = \hat{g}_i. \tag{4}$$

Assumptions (2)–(4) account for a broad class of saturable enzyme kinetics [13], e.g. a turnover rate of the form

$$g_i(s_{i-1}) = \frac{k_{\mathrm{cat\,i}} s_{i-1}^q}{K_{\mathrm{M\,i}} + s_{i-1}^q}, \tag{5}$$

can describe both irreversible Michaelis-Menten (for $q = 1$) and Hill-type (for $q > 1$) kinetics.

B. Transcriptional circuit

We model the rate of change of the enzyme concentrations as

$$\dot{e}_i = \kappa_i^0 + \kappa_i^1 \sigma_i(s_n) - \gamma e_i, \tag{6}$$

for $i = 1, 2, \ldots, n$. The equations in (6) come from the balance between protein synthesis and degradation (modeled as a linear process with kinetic constant $\gamma > 0$). The basal expression rate κ_i^0 describes the leaky expression of each enzyme, whereas the expression rate κ_i^1 represents the aggregate effect of promoter and ribosome binding site (RBS) strengths.

The function $\sigma_i(s_n)$ represents the feedback action of product-responsive TFs that repress protein expression. This kind of transcriptional feedback is common in natural regulatory mechanisms such as the tryptophan operon [11], and genetic control of amino acid metabolism [12]. Transcriptional repression allows for an increase in pathway flux by upregulating the enzymes in response to a larger demand for product. We model the regulatory effect of the product as a Hill function

$$\sigma_i(s_n) = \frac{\theta_i^{h_i}}{\theta_i^{h_i} + s_n^{h_i}}, \tag{7}$$

with Hill coefficients $h_i > 0$ and repression thresholds $\theta_i > 0$. The function σ_i is a lumped description of the regulatory effect. It does not describe the specific interaction between the product and the TFs, but instead represents the net effect of the product on the transcription rates.

Altogether, the model for the metabolic network under one-to-all negative regulation reads:

$$\begin{aligned}
&\dot{s}_i = g_i(s_{i-1})e_i - g_{i+1}(s_i)e_{i+1},\ i = 1, 2, \ldots, n-1,\\
&\dot{s}_n = g_n(s_{n-1})e_n - d,\\
&\dot{e}_i = \kappa_i^0 + \kappa_i^1 \frac{\theta_i^{h_i}}{\theta_i^{h_i} + s_n^{h_i}} - \gamma e_i,\ i = 1, 2, \ldots, n,
\end{aligned} \tag{8}$$

with a constant substrate s_0. In its current form, the model accounts for independent regulation of each gene (as in Fig. 1A). By taking identical regulatory functions $\sigma_i = \sigma$ for all i, the model can also describe operon control, whereby a set of genes are collectively transcribed in response to a single TF (as in Fig. 1B).

III. Existence of a steady state

A. Basal and maximal metabolic demand

We will denote the steady state metabolite concentrations, enzyme concentrations, and reaction rates as $\bar{s}_i$, $\bar{e}_i$ and $\bar{v}_i$, respectively. The steady state rates are

$$\bar{v}_i = g_i(\bar{s}_{i-1})\bar{e}_i, \tag{9}$$

and since the regulatory function is bounded as $\sigma_i(s_n) \in [0, 1)$, from (8) we observe that the steady state enzyme concentrations are bounded as $\bar{e}_i \in \left(E_i^{\mathrm{off}}, E_i^{\mathrm{on}}\right]$ with

$$E_i^{\mathrm{off}} = \frac{\kappa_i^0}{\gamma}, \qquad E_i^{\mathrm{on}} = \frac{\kappa_i^0 + \kappa_i^1}{\gamma}. \tag{10}$$

The input substrate s_0 is constant, and therefore the first reaction rate is bounded as $\bar{v}_1 \in \left(g_1(s_0)E_1^{\mathrm{off}}, g_1(s_0)E_1^{\mathrm{on}}\right]$. In steady state we have $\bar{v}_1 = g_1(s_0)\bar{e}_1 = d$, which can only be met if the metabolic demand satisfies $d \in (d_{\min}, d_{\max}]$ with

$$d_{\min} = g_1(s_0)E_1^{\mathrm{off}}, \qquad d_{\max} = g_1(s_0)E_1^{\mathrm{on}}. \tag{11}$$

B. Metabolite and enzyme equilibria

The relative steady state expression level

$$R_i = \frac{\bar{e}_i - E_i^{\mathrm{off}}}{E_i^{\mathrm{on}} - E_i^{\mathrm{off}}}, \tag{12}$$

quantifies the steady state enzyme concentration $\bar{e}_i$ needed to sustain a steady state relative to the basal and maximal expression levels. Since the enzyme steady state must lie within the bounds $\bar{e}_i \in \left(E_i^{\mathrm{off}}, E_i^{\mathrm{on}}\right]$, the relative expression must satisfy $R_i \in (0, 1]$. Setting $d = g_1(s_0)\bar{e}_1$ we obtain the expression level for the first enzyme

$$R_1(d) = \frac{d/g_1(s_0) - E_1^{\mathrm{off}}}{E_1^{\mathrm{on}} - E_1^{\mathrm{off}}}, \tag{13}$$

where we have explicitly denoted the dependence of the expression level R_1 on the demand d. Note that under the assumption that the demand satisfies $d \in (d_{\min}, d_{\max}]$, it

follows that $R_1(d) \in (0,1]$ and therefore a steady state for e_1 always exists.

We obtain the product steady state by setting $\dot{e}_1 = 0$:

$$\bar{s}_n = \theta_1 \sqrt[h_1]{\frac{1-R_1(d)}{R_1(d)}}, \tag{14}$$

which satisfies $\bar{s}_n \geq 0$ provided that $d \in (d_{\min}, d_{\max}]$. From the model equations in (8) we can also show that

$$R_i(d) = \frac{\theta_i^{h_i}}{\theta_i^{h_i} + \theta_1^{h_i}\left(\frac{1-R_1(d)}{R_1(d)}\right)^{h_i/h_1}}, \; i \geq 2. \tag{15}$$

In the special case of operon control (see Fig. 1B), we note that the relative expression levels take a simple form: for equal regulatory functions for every gene (i.e. $\theta_i = \theta_1$ and $h_i = h_1$ for all i), equation (15) simplifies to

$$R_i(d) = R_1(d), \; i \geq 2. \tag{16}$$

The general expression levels R_i in (15) satisfy $R_i(d_{\min}) = 0$, $R_i(d_{\max}) = 1$, and $R_i'(d) > 0$, which implies that $R_i(d) \in (0,1]$. Therefore, provided that the demand is in the range $d \in (d_{\min}, d_{\max}]$, a valid steady state for the enzymes $\bar{e}_i$ exists for any combination of positive parameters. In the case of the intermediate metabolites, however, the existence of a steady state is more subtle.

By setting $\bar{v}_i = d$ for $2 \leq i \leq n$ we obtain an algebraic equation for the intermediates

$$g_i(\bar{s}_{i-1}) = d/\bar{e}_i. \tag{17}$$

Although the monotonicity of g_i implies uniqueness of the metabolite steady state $\bar{s}_{i-1}$, equation (17) has a positive solution only if $d/\bar{e}_i < \hat{g}_i$, which is equivalent to

$$R_i(d) > \frac{d/\hat{g}_i - E_i^{\text{off}}}{E_i^{\text{on}} - E_i^{\text{off}}}, \tag{18}$$

where $\hat{g}_i$ is the saturation value defined in (4). From the inequality in (18) we see that enzyme saturation limits the parameter region that yields a positive steady state for the intermediate metabolites. Note that, in general, the expression levels in (15) may not satisfy condition (18). The next result gives a sufficient condition for the existence of a steady state.

Proposition 1 (Steady state under operon control): Assume that the demand satisfies $d \in (d_{\min}, d_{\max}]$. If the expression rates satisfy

$$\kappa_i^0 \hat{g}_i \geq \kappa_1^0 g_1(s_0), \qquad \kappa_i^1 \hat{g}_i > \kappa_1^1 g_1(s_0), \tag{19}$$

then the network (8) under operon control has a unique positive steady state.

Proof: We know that the existence of the enzymes $\bar{e}_i$ and product $\bar{s}_n$ is guaranteed by $d \in (d_{\min}, d_{\max}]$, whereas the intermediates depend on condition (18). Under operon control we have $R_i = R_1$ and therefore both sides of (18) are line segments in the (R_i, d) plane. By comparing the intercepts and slope of these line segments, we get the sufficient conditions in (19). ∎

From these results we observe two fundamental differences between operon and non-operon control. Firstly, in operon control the existence of a steady state depends on tuneable parameters such as promoter and RBS strengths (comprised in the parameters κ_i^1). In the case of non-operon control, however, the existence of a steady state also depends on the repression thresholds and Hill coefficients (because the shape of $R_i(d)$ depends critically on θ_i and h_i, recall (15)), both of which are generally difficult to modify experimentally. Therefore, considering the inherent cell-to-cell variability of genetic parameters, operon control appears to be more robust than non-operon control. Secondly, operon control yields equal relative expression levels (R_i), while non-operon control is more flexible in that it allows for fine-tuning the expression levels with different combinations of repression thresholds and/or Hill coefficients (see (15)).

These observations suggest a robustness/flexibility compromise between operon and non-operon control. We illustrate this compromise in Fig. 2 by plotting the expression levels $R_i(d)$ for different combinations of thresholds and Hill coefficients (the shaded area is the region where condition (18) is violated).

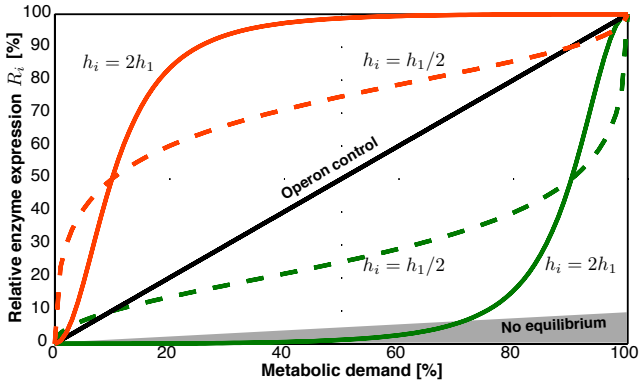

Fig. 2. Compromise between operon and non-operon regulation. (Black) Operon control yields uniform relative expression levels and the expression rates can be chosen to guarantee the existence of a steady state (see Proposition 1). Non-operon control allows for individual tuning of the expression levels, but the existence of the steady state also depends on the repression threshold and Hill coefficients. (Green) Non-operon with $\theta_i = \theta_1/3$. (Red) Non-operon regulation with $\theta_i = 3\theta_1$. In the shaded area the steady state of the intermediates does not exist (see (18)). The demand and the relative expression levels are in % of the ranges $(d_{\min}, d_{\max}]$ and $(E_i^{\text{off}}, E_i^{\text{on}}]$. The parameters for the first enzyme are $\kappa_1^0 = 0$, $\kappa_1^1 = 5$, $h_1 = 2$, and $\theta_1 = 3$. The remaining parameters are $s_0 = 1$, $\gamma = 1.2$, and we use Michaelis-Menten kinetics ($k_{\text{cat i}} = 100$ and $K_{\text{M i}} = 10$ for all i).

IV. Stability of an Operon Control Circuit

In this section we study the local stability of an operon control circuit for a given metabolic demand. Under an operon structure we take equal regulatory functions for every gene, i.e. we use $\sigma_i = \sigma$ with $h_i = h$ and $\theta_i = \theta$ for all i. Our analysis relies on the examination of the structure of the Jacobian matrix of (8), an approach that proved successful in earlier works (e.g. [15] for the case of metabolic pathways under product inhibition and linear kinetics). For a network with n metabolites and n enzymes, the Jacobian matrix

$J \in \mathbb{R}^{2n\times 2n}$ is

$$J = \begin{bmatrix} J_{11} & J_{12} \\ J_{21} & J_{22} \end{bmatrix}, \tag{20}$$

where the four blocks are $n \times n$ matrices given by

$$J_{11} = \begin{bmatrix} -a_2 & 0 & 0 & \cdots & 0 \\ a_2 & -a_3 & 0 & \cdots & 0 \\ 0 & a_3 & \ddots & \ddots & \vdots \\ \vdots & \ddots & \ddots & -a_n & \vdots \\ 0 & \cdots & \cdots & a_n & 0 \end{bmatrix}, \tag{21}$$

$$J_{12} = g_1(s_0) \begin{bmatrix} 1 & -\beta_2 & 0 & \cdots & 0 \\ 0 & \beta_2 & -\beta_3 & \cdots & 0 \\ 0 & 0 & \beta_3 & \ddots & \vdots \\ \vdots & \ddots & \ddots & \ddots & -\beta_n \\ 0 & \cdots & \cdots & \cdots & \beta_n \end{bmatrix}, \tag{22}$$

$$J_{21} = \sigma'(\bar{s}_n) \begin{bmatrix} 0 & \cdots & 0 & \kappa_1^1 \\ \vdots & \ddots & \ddots & \kappa_2^1 \\ \vdots & \ddots & \ddots & \vdots \\ 0 & \cdots & 0 & \kappa_n^1 \end{bmatrix}, \tag{23}$$

$$J_{22} = -\gamma I, \tag{24}$$

and we have defined

$$a_i = g_i'(\bar{s}_{i-1})\bar{e}_i, \tag{25}$$

$$\beta_i = \bar{e}_1/\bar{e}_i. \tag{26}$$

Note that because g_i is nondecreasing it follows that $a_i \geq 0$ for all i. With the above definitions, we have the next result.

Proposition 2 (Fixed modes under operon control): Under the conditions of Proposition 1, the linearized dynamics of (8) under operon control have $n-1$ stable fixed modes at $\lambda = -\gamma$.

Proof: With the partition in (20) the characteristic polynomial of J (i.e. $p(\lambda) = \det(J - \lambda I)$) can be written as

$$\begin{aligned} p(\lambda) &= \det(J_{22} - \lambda I) \times \\ &\quad \det\left((J_{11} - \lambda I) - J_{12} \left(J_{22} - \lambda I\right)^{-1} J_{21} \right), \\ &= (-1)^n (\lambda + \gamma)^n \det\left((J_{11} - \lambda I) + \frac{J_{12} J_{21}}{\lambda + \gamma} \right), \end{aligned} \tag{27}$$

where the product $J_{12}J_{21}$ is

$$J_{12}J_{21} = \begin{bmatrix} 0 & 0 & \cdots & r_1 \\ 0 & 0 & \cdots & r_2 \\ \vdots & \ddots & \ddots & \vdots \\ 0 & 0 & \cdots & r_n \end{bmatrix}, \tag{28}$$

and

$$\begin{aligned} r_i &= g_1(s_0)\sigma'(\bar{s}_n)\left(\beta_i \kappa_i^1 - \beta_{i+1}\kappa_{i+1}^1\right),\ i \leq (n-1), \\ r_n &= g_1(s_0)\sigma'(\bar{s}_n)\beta_n \kappa_n^1. \end{aligned} \tag{29}$$

From the structure of J_{11} and the product $J_{12}J_{21}$, we can carry one $(\lambda+\gamma)$ term into the determinant in (27) and then into the last column of its argument. This leads to

$$p(\lambda) = (\lambda + \gamma)^{n-1} \bar{p}(\lambda), \tag{30}$$

where the factor $\bar{p}(\lambda)$ is a polynomial given by

$$\bar{p}(\lambda) = \det\left(\begin{bmatrix} (\lambda + a_2) & 0 & \cdots & -r_1 \\ -a_2 & \ddots & \cdots & \vdots \\ \vdots & \ddots & (\lambda + a_n) & -r_{n-1} \\ 0 & \cdots & -a_n & \lambda(\lambda+\gamma) - r_n \end{bmatrix} \right), \tag{31}$$

From (30) we conclude that $p(\lambda)$ has $(n-1)$ roots at $\lambda = -\gamma < 0$. These eigenvalues are independent of the parameters of the genetic control circuit, and therefore they are fixed modes of the feedback system. Note that if $\bar{p}(-\gamma) = 0$, then the Jacobian has additional eigenvalues at $\lambda = -\gamma$, but these are not fixed modes because $\bar{p}(-\gamma) = 0$ holds only under specific combinations of the constants r_i, which in turn depend on the feedback parameters (namely the expression rates and Hill function, see (29)). ■

Enzyme degradation rates are inversely proportional to their half-lives, which are much longer than metabolic time scales (half-lives are in the order of minutes to hours, whereas metabolic time scales are typically milliseconds to seconds [13]) . The fixed modes in Proposition 2 therefore correspond to an upper bound on the response speed that a one-to-all control circuit can provide.

The remaining $n+1$ modes of the feedback system are the roots of the polynomial $\bar{p}(\lambda)$ given in (31). The location of these depends in an intricate way on the expression rates, the regulatory function σ, and the metabolic demand. We numerically find that there are parameter combinations that lead to local instability (see Fig. 3A–C). In the full nonlinear system, the locally unstable region is defined by two Hopf bifurcations (Fig. 3D) between which the system displays a stable limit cycle. From Fig. 3A–C we observe a higher Hill coefficient tends to enlarge the region for the existence of a limit cycle. This is not surprising in view that switch-like control is typically more prone to oscillations.

The numerical results in Fig. 3 suggest that basal enzyme expression plays a key role on the emergence of local instability. Under local instability the control circuit is unable to supply the cellular demand for product and enters an oscillatory regime. However, as shown in the next result, local instability can be ruled out when the basal expression is negligible.

Proposition 3 (Stability under nil basal expression): Under the conditions of Proposition 1 and in the absence of basal expression, i.e. $\kappa_i^0 = 0$ for all i, the operon-controlled network is locally stable.

Proof: We know that the Jacobian of (8) has $n-1$ stable eigenvalues at $\lambda = -\gamma$, and that the remaining eigenvalues are the roots of $\bar{p}(\lambda)$ given in (31).

Under operon control the relative expression levels are the same for each enzyme (recall (16)), i.e. $R_i = R_1, i \geq 2$.

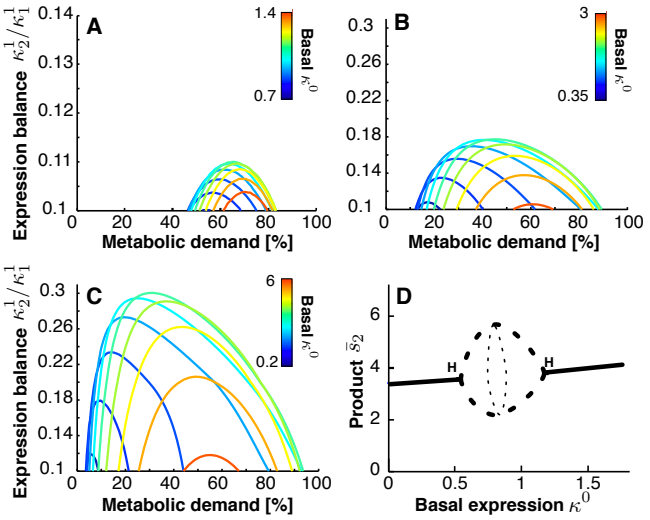

Fig. 3. Effect of the genetic parameters and the metabolic demand on the emergence of stable oscillations under operon regulation. (A–C) Stability region for a pathway of length $n = 2$ as a function of the basal expression rate $\kappa^0 = \kappa_1^0 = \kappa_2^0$, the expression balance ratio κ_2^1/κ_1^1 with $\kappa_1^1 = 10$, and Hill coefficient ($h = \{2, 4, 8\}$ in panels A, B, and C, respectively); the demand is shown in % of the range $(d_{\min}, d_{\max}]$. In the region under the curves some of the eigenvalues of the Jacobian have positive real parts; the stability regions were computed with the Routh-Hurwitz criterion applied to $\bar{p}(\lambda)$. (D) Bifurcation diagram of the nonlinear model (8): steady state product concentration $\bar{s}_2$ as a function of the basal expression rate κ^0 (Hopf bifurcations marked as H). The bifurcation diagram was computed with Matcont for Matlab [16]. The substrate, regulatory thresholds, enzyme kinetics and degradation rates are those used in Fig. 2.

Using the definition of R_i in (12) we can therefore write the ratio $\beta_i = \bar{e}_1/\bar{e}_i$ as

$$\beta_i = \frac{(E_1^{\text{on}} - E_1^{\text{off}})R_1(d) + E_1^{\text{off}}}{(E_i^{\text{on}} - E_i^{\text{off}})R_1(d) + E_i^{\text{off}}}. \tag{32}$$

In the absence of basal expression ($\kappa_i^0 = 0$), the OFF expression levels are also nil ($E_i^{\text{off}} = 0$), so that β_i becomes

$$\beta_i = E_1^{\text{on}}/E_i^{\text{on}} = \kappa_1^1/\kappa_i^1, \tag{33}$$

and therefore the constants r_i in (29) simplify to $r_i = 0$ for all $i \neq n$. Substituting $r_i = 0, i \neq n$, in (31) the polynomial $\bar{p}(\lambda)$ is given by the determinant of a lower bidiagonal matrix, namely

$$\bar{p}(\lambda) = \prod_{i=2}^{n} (\lambda + a_i)\left(\lambda(\lambda + \gamma) - r_n\right). \tag{34}$$

From (34) we conclude that the Jacobian has $(n-1)$ real and stable eigenvalues at $\lambda = -a_i < 0$, for $i = 2, 3, \ldots, n$, and two complex eigenvalues at

$$\lambda_{1,2} = \left(-\gamma \pm \sqrt{\gamma^2 + 4\kappa_1^1 \sigma'(\bar{s}_n) g_1(s_0)}\right)/2. \tag{35}$$

The eigenvalues $\lambda_{1,2}$ are also stable because $\sigma'(\bar{s}_n) < 0$ implies that the polynomial $(\lambda(\lambda + \gamma) - r_n)$ has positive coefficients, and therefore its roots satisfy $\Re\{\lambda_{1,2}\} < 0$. Note that this holds for any regulatory function that is monotonically decreasing, not necessarily Hill-type. ■

V. Dynamic response of an operon circuit

In the previous sections we focused on the behavior of the genetic circuit for a fixed metabolic demand. Synthetic circuits, however, operate in dynamic environments whereby cell demands may change due to resource reallocation, environmental stimuli, or the activity of other synthetic circuits. Another key function of the genetic control circuit is therefore to dynamically modulate enzyme concentrations in a way that the pathway flux adapts to changes in the demand for product. We will consider an abrupt change in the metabolic demand

$$d(t) = \begin{cases} d^i & t \leq t^* \\ d^f & t > t^* \end{cases}, \tag{36}$$

where both demand values are in the allowed range $\{d^i, d^f\} \subset (d_{\min}, d_{\max}]$. We consider the case of operon regulation, and since our interest is on the transient adaptation of the pathway, we assume that the regulatory circuit has been designed to be stable for both demand levels, and that the complete system is in steady state at $t = t^*$.

Although stability is sufficient for the system to reach the new demand, the transient *performance* depends on the fine-tuning of the transcriptional parameters and the size of the demand change (i.e. $|d^f - d^i|$). In Fig. 4 we plot different transient responses for a range of expression rates κ_1^1. We observe that after the transient, the first reaction rate matches the new demand. The response speed can be fine-tuned with κ_1^1 and we achieve the fastest response with $\kappa_1^1 \approx 0.5$, with no further improvements for values $\kappa_1^1 < 0.5$ (not shown). This behavior is in agreement with Proposition 2, as the fastest response in Fig. 4 (blue line) has a time constant that matches the inverse of the enzyme degradation rate.

From Fig. 4 we also see that the post-stimuli steady state product concentration is sensitive to the chosen expression rate. This sensitivity translates into a performance tradeoff between the transient speed and the steady state product bias: faster responses can be achieved at the expense of a larger bias, and *vice versa*. The bias is an unwanted feature, as one would ideally seek for a "perfect" adaptation whereby metabolites return to their pre-stimulus level. Next we examine the effect of the transcriptional parameters on the bias of the intermediate metabolites and product.

a) Steady state bias of the intermediates: Upon a demand change, the relative enzyme levels change from $R_1(d^i)$ to $R_1(d^f)$, and from equation (17) we know that the steady state for each intermediate is given by

$$\bar{s}_{i-1}^f = g_i^{-1}\left(g_1(s_0)\beta_i^f\right), \tag{37}$$

where $\beta_i^f = \bar{e}_1^f/\bar{e}_i^f$ and we have used the fact that in steady state $d^f = g_1(s_0)\bar{e}_1^f$. Recalling (32) we have that

$$\beta_i^f = \frac{(E_1^{\text{on}} - E_1^{\text{off}})R_1(d^f) + E_1^{\text{off}}}{(E_i^{\text{on}} - E_i^{\text{off}})R_1(d^f) + E_i^{\text{off}}}. \tag{38}$$

From the above we conclude that $\bar{s}_{i-1}^f$ depends on the new demand, but this dependency disappears in the absence of

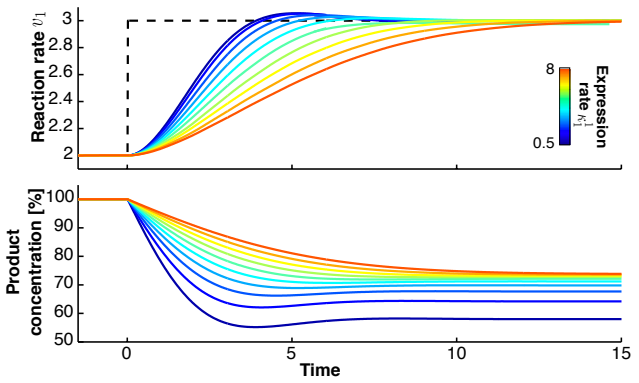

Fig. 4. Transient responses after a 50% step increase in product demand (dashed line). Pathway of length $n = 2$ under operon regulation; the circuit is stable for the whole range of κ_1^1 with nonzero basal expression $\kappa_1^0 = \kappa_2^0 = 0.1$. The remaining transcriptional parameters are $\kappa_2^1 = 4$, $\theta = 3$, $h = 2$, with enzyme degradation rate $\gamma = 1.2$. The substrate and enzyme kinetics are identical to those in Fig. 2. Product concentration shown in % of its pre-stimulus level.

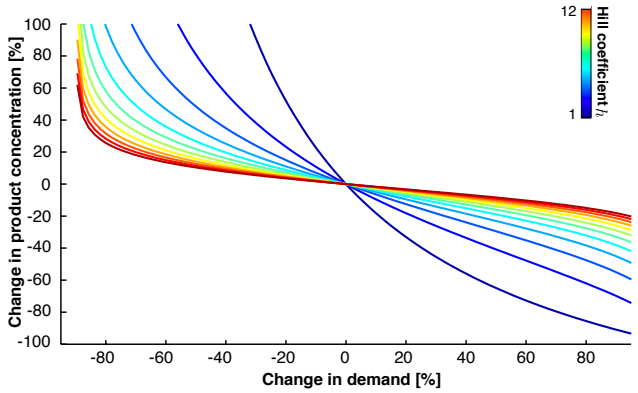

Fig. 5. Effect of demand and Hill coefficient on the product bias after a change in demand. Model parameters are those of Fig. 4 with $\kappa_1^1 = 2$ and initial demand $d^i = (d_{\max} - d_{\min})/2$; the change in demand and product concentration are plotted in % of their pre-stimulus levels.

basal enzyme expression (in which case β_i^f simplifies to $\beta_i^f = \kappa_1^1/\kappa_i^1$). For nonzero basal expression, the sensitivity $\partial \bar{s}_{i-1}^f / \partial d^f$ can be fine-tuned with the expression rates κ_i^1, whereas nil basal expression translates into perfect adaptation of the intermediates.

b) Steady state bias of the product: From the expression in (14), we know that under operon regulation the post-stimulus product steady state is

$$\bar{s}_n^f = \theta \sqrt[h]{\left(1 - R_1(d^f)\right)/R_1(d^f)}, \tag{39}$$

which indicates that the product bias depends not only on the new demand d^f, but also on the Hill coefficient and repression threshold. For low Hill coefficients, the product steady state can be highly dependent on the demand. However, the sensitivity $\partial \bar{s}_n^f / \partial d^f$ in (39) decreases with increasing h (see Fig. 5), and therefore the regulatory steepness can be used to curb the compromise between product bias and response time (observed previously in Fig. 4). Since a steeper regulation also shrinks the stability region (see Fig. 3), the circuit performance is subject to a tradeoff between its ability to match the cellular demand and the steady state product bias.

VI. Outlook

We have explored the ability of a one-to-all genetic control circuit to adapt enzyme concentrations in a way that the pathway flux matches the cellular demand for product. The analysis has revealed a number of design tradeoffs between stability, response speed, and steady state metabolite bias. We are working on a number of extensions to this work. These aim primarily at: (a) identifying how the tradeoffs can be mitigated by increasing the complexity of the feedback (e.g. by considering more complex gene-metabolite pairings and combinations of repression/activation loops), and (b) extending the analysis to more complex metabolic pathways.

The wetlab implementation of genetic-metabolic circuits, let alone parameter fine-tuning, can be costly and time consuming. Our work provides useful insights into which factors need to be addressed at a design stage, potentially facilitating the implementation with a model-guided rationale.

References

[1] M. B. Elowitz and S. Leibler, "A synthetic oscillatory network of transcriptional regulators," *Nature*, vol. 403, no. 6767, pp. 335–338, Jan. 2000.

[2] T. S. Gardner, C. R. Cantor, and J. J. Collins, "Construction of a genetic toggle switch in Escherichia coli," *Nature*, vol. 403, no. 6767, pp. 339–342, Jan. 2000.

[3] T. K. Lu, A. S. Khalil, and J. J. Collins, "Next-generation synthetic gene networks." *Nature biotechnology*, vol. 27, no. 12, pp. 1139–50, Dec. 2009.

[4] W. J. Holtz and J. D. Keasling, "Engineering static and dynamic control of synthetic pathways." *Cell*, vol. 140, no. 1, pp. 19–23, Jan. 2010.

[5] P. E. M. Purnick and R. Weiss, "The second wave of synthetic biology: from modules to systems." *Nature reviews. Molecular cell biology*, vol. 10, no. 6, pp. 410–22, June 2009.

[6] W. R. Farmer and J. C. Liao, "Improving lycopene production in Escherichia coli by engineering metabolic control," *Nat Biotech*, vol. 18, no. 5, pp. 533–537, May 2000.

[7] E. Fung, *et al.*, "A synthetic gene-metabolic oscillator," *Nature*, vol. 435, no. 7038, pp. 118–122, May 2005.

[8] N. Anesiadis, W. R. Cluett, and R. Mahadevan, "Dynamic metabolic engineering for increasing bioprocess productivity," *Metabolic Engineering*, vol. 10, no. 5, pp. 255–266, Sept. 2008.

[9] M. J. Dunlop, J. D. Keasling, and A. Mukhopadhyay, "A model for improving microbial biofuel production using a synthetic feedback loop," *Systems and Synthetic Biology*, vol. 4, no. 2, pp. 95–104, 2010.

[10] D. A. Oyarzún, M. Chaves, and M. Hoff-Hoffmeyer-Zlotnik, "Multistability and oscillations in genetic control of metabolism." *Journal of Theoretical Biology*, vol. 295, pp. 139–153, 2012.

[11] M. Santillán and M. C. Mackey, "Dynamic regulation of the tryptophan operon: A modeling study and comparison with experimental data," *Proceedings of the National Academy of Sciences of the United States of America*, vol. 98, no. 4, pp. 1364–1369, Feb. 2001.

[12] A. Zaslaver, *et al.*, "Just-in-time transcription program in metabolic pathways," *Nature Genetics*, vol. 36, no. 5, pp. 486–491, May 2004.

[13] A. Cornish-Bowden, *Fundamentals of Enzyme Kinetics*, 3rd ed. Portland Press, 2004.

[14] R. Heinrich and S. Schuster, *The regulation of cellular systems*. Chapman & Hall, 1996.

[15] J. Tyson and H. Othmer, "The dynamics of feedback control circuits in biochemical pathways," *Progress in Theoretical Biology*, vol. 5, pp. 1–62, 1978.

[16] W. Govaerts and Y. Kuznetsov, "MatCont: continuation software in Matlab," http://www.matcont.ugent.be/.